Title

ActiveBAS: A Low-cost, Scalable Control Solution for Grid-Interactive Small and Medium Sized Commercial Buildings

Authors

Kim, Donghun

Ham, Sang Woo

Publication Date

2023-09-08

DOI

10.2172/1998953

Peer reviewed

Building Technologies & Urban Systems Division
Energy Technologies Area
Lawrence Berkeley National Laboratory

ActiveBAS: A Low-cost, Scalable Control Solution for Grid-Interactive Small and Medium Sized Commercial Buildings (CRADA Final Report)

Donghun Kim, Sang woo Ham

Energy Technologies Area
September 2023

10.2172/1998953

This work was supported by the Assistant Secretary for Energy Efficiency and Renewable Energy,
Building Technologies Office, of the US Department of Energy
under Contract No. DE-AC02-05CH11231.

Disclaimer:

ActiveBAS: A Low-cost, Scalable Control Solution for Grid-Interactive Small and Medium Sized Commercial Buildings

Donghun Kim[a], Sang Woo Ham[a]

[a]*Building Technology & Urban System Division, Lawrence Berkeley National Laboratory, Berkeley, CA,*

Abstract

This project aims to develop and enhance a low-cost, highly scalable control solution for Small and Medium-Sized Commercial Buildings (SMCB), assess the business potential at multiple sites, and perform commercialization efforts. The technology can be applied to any buildings served by multiple units, with the benefits being greatest for open-spaced buildings, such as banks, retail stores, restaurants, and factories. This project aims to develop an affordable control solution for: 1) SMCB grid responsiveness, 2) reduction of GHG by changing unit operations, 3) greater reduction in utility costs, and 4) rapid adoption in the marketplace. The proposed technology will be built on a previously developed and demonstrated MPC solution. The minimal sensor requirement and less need of control expertise are the unique feature of the algorithm that leads to low capital and maintenance costs, and short installation and implementation time. These attributes contribute to low capital and maintenance costs, as well as a short installation and implementation time. However, these advantages come with a trade-off: increased difficulties and unreliability when applying traditional modeling and MPC control approaches due to limited information. This final report describes the modeling approaches developed and tested to overcome these challenges. It begins by outlining the modeling challenge posed by minimal sensor requirements, then delves into the proposed modeling approaches, which primarily involve system identification. Finally, preliminary test results for a simulation case study are presented.

1. Introduction

For real buildings, the information of various heat gains, such as lighting load, plug load, occupancy load and in/exfiltration, is often not available, and adding additional sensors to measure them for control purposes is cost prohibitive, especially for small and medium-sized commercial buildings. The imperfect building data set due to unmeasured heat gains (or unmeasured disturbances) often leads to failure of the conventional system identification approach (CONV) [1, 2], which minimizes a norm of errors between simulation and measurement, despite its popularity in the literature [3, 4]. This is because physical parameters such as thermal resistances and capacitances of a building thermal network model have to be biased to explain the input and output relationship without the unknown heat gains.

The biased estimation of capacitances and resistances for building's structural mass (e.g., concrete slab) is equivalent to over- or under-estimate the size or capacity of an electrochemical battery, since the mass itself is the thermal energy storage. Therefore, the poor estimation for the thermal energy storage degradates MPC performance significantly by making MPC to predict wrong charging/discharging rates and the amount of energy that can be stored, and could lead to even higher utility cost and less load flexibility.

It is critically important to develop different identification approaches that can extract a reasonable building model from imperfect measurements to overcome this problem. We provide a simulation case study to show how the conventional identification algorithm poorly behaves under unmeasured disturbances, and propose and compare alternative identification algorithms to overcome this issue. The proposed algorithms model not only the thermal dynamics of a building envelope system but also the dynamics of unmeasured disturbances in the form of either a lumped input disturbance (ID) [5, 6] or output disturbance (OD) [3, 4].

2. Comparisons of identification approaches under unmeasured disturbance and effect on prediction: simulation case study

2.1. True system description and data generation

It is very difficult to compare the performance of identification approaches for a real building since we do not know the true system dynamics or parameters. Instead, we created a hypothetical building envelope model and treated it as the *True model* for this study. The True model was tuned with a

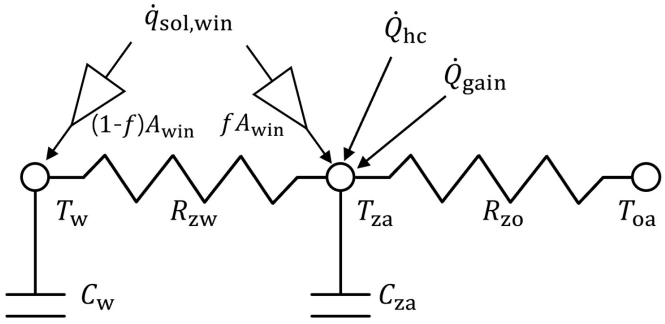

Figure 1: A simple RC network model for a case study building.

data set that was generated from a laboratory environment (FLEXLAB) [7] and that includes complete measurements of plug, lighting, and occupancy loads. The laboratory represents a single-zone office space. The True model has the RC network shown in Fig. 1 and the state-space form of Eq. 1 (state transition process) and Eq. 2 (measurement process).

$$\underbrace{\begin{bmatrix}\dot{T}_{\text{w}}\\ \dot{T}_{\text{za}}\end{bmatrix}}_{\dot{\mathbf{x}}} = \underbrace{\begin{bmatrix}\frac{-1}{C_{\text{w}}R_{\text{zw}}} & \frac{1}{C_{\text{w}}R_{\text{zw}}}\\ \frac{-1}{C_{\text{za}}R_{\text{zw}}} & \frac{-1}{C_{\text{za}}R_{\text{zw}}}+\frac{-1}{C_{\text{za}}R_{\text{zo}}}\end{bmatrix}}_{\mathbf{A}}\underbrace{\begin{bmatrix}T_{\text{w}}\\ T_{\text{za}}\end{bmatrix}}_{\mathbf{x}} + \underbrace{\begin{bmatrix}0 & \frac{(1-f)A_{\text{win}}}{C_{\text{w}}} & 0 & 0\\ \frac{1}{C_{\text{za}}R_{\text{zo}}} & \frac{fA_{\text{win}}}{C_{\text{za}}} & \frac{1}{C_{\text{za}}} & \frac{1}{C_{\text{za}}}\end{bmatrix}}_{\mathbf{B}}\underbrace{\begin{bmatrix}T_{\text{oa}}\\ \dot{q}_{\text{sol,win}}\\ \dot{Q}_{\text{hc}}\\ \dot{Q}_{\text{gain}}\end{bmatrix}}_{\mathbf{u}} \tag{1}$$

$$y_{\text{za}} = \underbrace{\begin{bmatrix}0 & 1\end{bmatrix}}_{\mathbf{C}}\mathbf{x} \tag{2}$$

- T_{w}, T_{za}, and T_{oa} are temperature nodes of large thermal mass (w), zone air (za), and outdoor air (oa)
- R_{zw} and R_{zo} are thermal resistances between temperature nodes [K/kW]
- C_{w} and C_{za} are thermal capacitances [kWh/K]

- $\dot{q}_{\text{sol,win}}$ is incident solar radiation per area on windows [kW/m^2], A_{win} is effective window area [m^2]
- f is convective fraction of the incident solar radiation
- $\dot{Q}_{\text{hc}}$ is heating/cooling rate from maximum heating rate ($\dot{Q}_{\text{hc,max}}$) to maximum cooling rate ($-\dot{Q}_{\text{hc,max}}$) [kW]
- $\dot{Q}_{\text{gain}}$ is the summation of plug, lighting, and occupancy loads [kW]
- y_{za} is measured zone air temperature [°C]

The parameters to be estimated through the system identification are $\theta = [C_{\text{w}}, C_{\text{za}}, R_{\text{zw}}, R_{\text{zo}}, f, A_{\text{win}}]$ and were tuned with the complete measurements including $\dot{Q}_{\text{gain}}$. The values of the True model were set to C_{w}: 2.5 kWh/K, C_{za}: 0.67kWh/K, R_{zw}: 1.8 K/kW, R_{zo}: 18 K/kW, f: 0.2, and A_{win}: 4.5 m^2. A proportional-integral (PI) controller modulates heating or cooling rate ($\dot{Q}_{\text{hc}}$) to maintain indoor temperature, and the maximum heating and cooling rates are 6 kW and -6 kW, respectively.

To test performance of the identification algorithms of the CONV, ID and OD under a practical scenario, $\dot{Q}_{\text{gain}}$ is assumed to be unknown. Instead, it is assumed that we can design experiments and actively control indoor temperature setpoint (within an acceptable room air temperature band) for the purpose of better system identification. Two weeks of a data set was generated from the True model with Oakland, CA weather data [8]. During the weekdays, cooling setpoint is set to 23°C-25°C for occupied times ($6-19$ hour) and 28°C-30°C for the unoccupied time, but the setpoint of the first weekend (2 days) was perturbed according to a pseudo binary random signal (PRBS) with 2 hour of time-scale and 4th order. The binary signal was mapped to sampled setpoints between $18-25$°C. The generated data set is visualized in Fig. 2.

2.2. Descriptions of system identification approaches

Eqs. 1-2 were discretized with a 5-min sampling time by using the zero-order hold [9]. Three different system identification approaches (CONV, ID, and OD) were tested with the test data set aiming at identifying the True model. They have the same model structure of the discretized system model for the building envelope dynamics although their disturbance model structures differ. Note that unmeasured disturbance ($\dot{Q}_{\text{gain}}$) was not provided

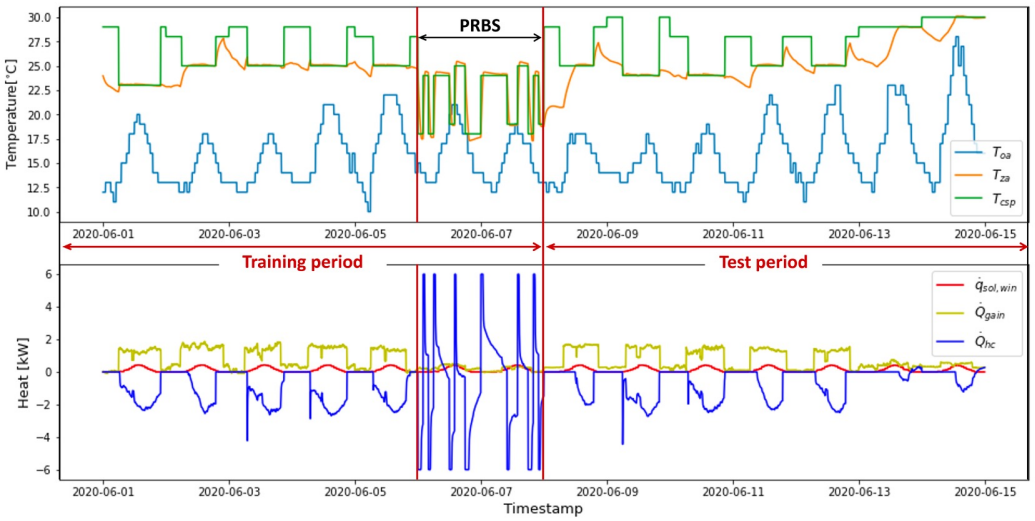

Figure 2: Test data set of temperatures (T_{oa}:outdoor air temp. T_{za}: zone air temp. T_{csp}: room cooling setpoint) and measured/unmeasured disturbances to evaluate performance of different identification algorithms.

to the identification algorithms. In other words, the identified model G maps only the measured disturbances (T_{oa}, $\dot{q}_{\mathrm{sol,win}}$) and control input ($\dot{Q}_{\mathrm{hc}}$) to the indoor air temperature (y_{za}).

2.2.1. Conventional simulation error minimization approach

The CONV approach assumes that all the unmeasured disturbance can be expressed as white noise (e_{conv}) in the measurement process, and the discretized system can be written as Eq. (3);

$$\begin{aligned} \mathbf{x}(k+1) &= \mathbf{A}_{\mathrm{d}}\mathbf{x}(k) + \mathbf{B}_{\mathrm{d}}\mathbf{u}(k) \\ y(k) &= \mathbf{C}_{\mathrm{d}}\mathbf{x}(k) + e_{\mathrm{conv}}(k) \end{aligned} \tag{3}$$

where $\mathbf{A}_{\mathrm{d}}$, $\mathbf{B}_{\mathrm{d}}$, and $\mathbf{C}_{\mathrm{d}}$ from $\mathbf{A}$, $\mathbf{B}$, and $\mathbf{C}$ in Eqs. (1)-(2).

The set of parameters (θ^*_{conv}) is estimated by minimizing the sum of squared errors between simulation ($\hat{y}(k;\theta) = \mathbf{C}_{\mathrm{d}}\hat{\mathbf{x}}(k;\theta)$) and measurement ($y(k)$) via the nonlinear optimization (Eqs. 4-5);

$$\begin{aligned} \hat{\mathbf{x}}(k+1;\theta) &= \mathbf{A}_{\mathrm{d}}(\theta)\hat{\mathbf{x}}(k;\theta) + \mathbf{B}_{\mathrm{d}}(\theta)\mathbf{u}(k) \\ y(k) &= \mathbf{C}_{\mathrm{d}}\hat{\mathbf{x}}(k;\theta) + \varepsilon_{\mathrm{conv}}(k;\theta) \end{aligned} \tag{4}$$

$$\theta^{*}_{\text{conv}} = \arg\min_{\theta} \sum_{k=1}^{N} \left(\varepsilon_{\text{conv}}(k;\theta)\right)^2, \tag{5}$$

where subscript d indicates a discretized system and, k is a time step.

In the 7-day of training data, the initial state (i.e., $\mathbf{x}(0)$) is obtained via Kalman filter by using the first day data. Then, the following 6 days are predicted via simulation (Eqs. 4-5). The optimization bounds of parameters are set to [0.1, 50] for all R and C parameters (i.e., $C_{\text{w}}, C_{\text{za}}, R_{\text{zw}}, R_{\text{zo}}$), [1e-6, 1] for f, and [0.5, 25] for A_{win}.

2.2.2. Input disturbance identification approach

The ID approach assumes that unmeasured disturbances come from the input channel, i.e., the heat gain term, and treats the input disturbance as an additional dynamic state. This can be written as an augmented state space format (Eq. 6) [5, 6].

$$\begin{aligned} \underbrace{\begin{bmatrix} \dot{\mathbf{x}} \\ \dot{\zeta}_{\text{ID}} \end{bmatrix}}_{\dot{\mathbf{x}}_{\text{ID}}} &= \underbrace{\begin{bmatrix} \mathbf{A} & \mathbf{A}_{\zeta_{\text{ID}}} \\ \mathbf{0} & \mathbf{0} \end{bmatrix}}_{\mathbf{A}_{\text{ID}}} \underbrace{\begin{bmatrix} \mathbf{x} \\ \zeta_{\text{ID}} \end{bmatrix}}_{\mathbf{x}_{\text{ID}}} + \mathbf{B}\mathbf{u} + \mathbf{w}_{\text{ID}}, \text{ and } \mathbf{A}_{\zeta_{\text{ID}}} = \begin{bmatrix} \mathbf{0} \\ \frac{1}{C_{\text{za}}} \end{bmatrix} \\ y_{\text{za}} &= \underbrace{\begin{bmatrix} \mathbf{C} & 0 \end{bmatrix}}_{\mathbf{C}_{\text{ID}}} \mathbf{x}_{\text{ID}} + e_{\text{ID}} \end{aligned} \tag{6}$$

where $\mathbf{w}_{\text{ID}}$ and e_{ID} are state and measurement noises. ζ_{ID} represents the lumped input disturbance term.

The key idea in this approach is to treat ζ_{ID} as Wiener process, so therefore , it behaves as the Brownian motion after discretization according to its noise level (i.e., $\zeta_{\text{ID}}(k+1) = \zeta_{\text{ID}}(k) + w_{\zeta_{\text{ID}}}(k)$).

For the system identification, the ID approach firstly calculates one-step ahead prediction errors. The prediction errors are calculated via following steps. After discretizing the system in Eq. 6, it can be written as Eq. 7. From the initial states ($\hat{\mathbf{x}}_{\text{ID}}(1|1)$), the next time states ($\hat{\mathbf{x}}_{\text{ID}}(2|1)$) and zone air temperature ($\hat{y}_{\text{za}}(2|1)$) are predicted through Eq. 7. The prediction error (i.e., innovation, ε_{ID}) is estimated through Eq. 8, and then, the predicted states are updated by using the innovation and optimal Kalman gain ($\mathbf{K}(k)$) (Eq. 9). The process in Eqs. 7-9 is sequentially repeated for the whole data ($k = 1, 2, ..., N$). At each time k, the optimal Kalman gain can be obtained via Kalman filter [9]. The optimal Kalman gain is estimated based on state noise covariance ($\mathbf{\Sigma}_{\mathbf{x}_{\text{ID}}}$, i.e., $\mathbf{w}_{\text{ID}}(k) \sim N(0, \mathbf{\Sigma}_{\mathbf{x}_{\text{ID}}})$) and measurement

noise covariance $\mathbf{\Sigma}_{y_{\text{za}}}$ in the discretized system. While measurement noise covariance set to $0.25^2/T_s$ based on sensor noise (± 0.5°C) and discretization sampling time, T_s, the state noise variance is modeled by two additional parameters (i.e., $\mathbf{\Sigma}_{\mathbf{x}_{\text{ID}}} = \text{diag}(\sigma_x^2, \sigma_x^2, \sigma_{\zeta_{\text{ID}}}^2)$) that determine the movement level of update in $\hat{\mathbf{x}}_{\text{ID}} = [\hat{\mathbf{x}}, \hat{\zeta}_{\text{ID}}]^\intercal$ (Eq. 9). The optimization bound of the two parameters are set to [1e-4, 1].

$$\begin{aligned} \hat{\mathbf{x}}_{\text{ID}}(k+1|k;\theta) &= \mathbf{A}_{\text{d,ID}}(\theta)\hat{\mathbf{x}}_{\text{ID}}(k|k) + \mathbf{B}_{\text{d}}(\theta)\mathbf{u}(k) \\ \hat{y}_{\text{za}}(k+1|k;\theta) &= \mathbf{C}_{\text{d,ID}}\hat{\mathbf{x}}_{\text{ID}}(k+1|k) \end{aligned} \tag{7}$$

$$\varepsilon_{\text{ID}}(k+1;\theta) = y_{\text{za}}(k+1) - \hat{y}_{\text{za}}(k+1|k;\theta) \tag{8}$$

$$\hat{\mathbf{x}}_{\text{ID}}(k+1|k+1;\theta) = \hat{\mathbf{x}}_{\text{ID}}(k+1|k;\theta) + \mathbf{K}(k+1;\theta)\varepsilon_{\text{ID}}(k+1;\theta) \tag{9}$$

The ID approach finds a set of parameters by minimizing the square sum of one-step ahead prediction error (Eq. 10).

$$\theta_{\text{ID}}^* = \arg\min_{\theta} \sum_{k=1}^{N} \left(\varepsilon_{\text{ID}}(k;\theta)\right)^2 . \tag{10}$$

2.2.3. Output disturbance identification approach

The OD approach [3, 4] does not directly model the input disturbances. Instead, it tries to model the effect of unmeasured heat gains on the output (i.e., room air temperature). The aggregated contribution of the unknown heat sources to the output is called the output disturbance as opposed to the input disturbance. The OD approach models the output disturbance as a filtered process of white noise ($e_{\text{OD}}(k)$), which is called output disturbance ($v_{\text{OD}}(k)$ in Eq. 11). The output disturbance dynamics can be modeled with two more parameters, ρ_1 and ρ_2 (Eq. 11).

$$\begin{aligned} \mathbf{x}(k+1) &= \mathbf{A}_{\text{d}}\mathbf{x}(k) + \mathbf{B}_{\text{d}}\mathbf{u}(k) \\ y(k) &= \mathbf{C}_{\text{d}}\mathbf{x}(k) + v_{\text{OD}}(k) \\ \zeta_{\text{OD}}(k+1) &= \underbrace{[\rho_1]}_{\mathcal{F}}\zeta_{\text{OD}}(k) + \underbrace{[\rho_2]}_{\mathcal{G}}e_{\text{OD}}(k) \\ v_{\text{OD}}(k) &= \zeta_{\text{OD}}(k) + e_{\text{OD}}(k) \end{aligned} \tag{11}$$

The OD approach estimates a set of parameters by minimizing the square sum of one-step ahead prediction error (Eqs. 12-13). The optimization of bounds of ρ_1 and ρ_2 are set to [-0.999, 0.999] [3].

$$\begin{aligned}
\hat{\mathbf{x}}(k+1;\theta) &= \mathbf{A}_{\mathrm{d}}(\theta)\hat{\mathbf{x}}(k;\theta) + \mathbf{B}_{\mathrm{d}}(\theta)\mathbf{u}(k) \\
y(k) &= \mathbf{C}_{\mathrm{d}}\hat{\mathbf{x}}(k;\theta) + \hat{v}_{\mathrm{OD}}(k;\theta) \\
\hat{\zeta}_{\mathrm{OD}}(k+1;\theta) &= \mathcal{F}(\theta)\hat{\zeta}_{\mathrm{OD}}(k;\theta) + \mathcal{G}(\theta)\varepsilon_{\mathrm{OD}}(k) \\
\hat{v}_{\mathrm{OD}}(k;\theta) &= \hat{\zeta}_{\mathrm{OD}}(k;\theta) + \varepsilon_{\mathrm{OD}}(k;\theta)
\end{aligned} \tag{12}$$

$$\theta^*_{\mathrm{OD}} = \arg\min_{\theta} \sum_{k=1}^{N} \left(\varepsilon_{\mathrm{OD}}(k;\theta)\right)^2 \tag{13}$$

2.3. System identification results and discussion

For each identification algorithm, the optimization problem is non-convex, and hence to find a better optimal solution, we randomly sampled initial starting points and repeatedly solved the optimization problems for 50 times. The estimation results of CONV, ID, OD identification approaches are summarized in Table 1.

Table 1: Comparison of estimated parameters from system identification approaches

	C_{w} $[\frac{\mathrm{kWh}}{\mathrm{K}}]$	C_{za} $[\frac{\mathrm{kWh}}{\mathrm{K}}]$	R_{zw} $[\frac{\mathrm{K}}{\mathrm{kW}}]$	R_{zo} $[\frac{\mathrm{K}}{\mathrm{kW}}]$	f [-]	A_{win} $[\mathrm{m}^2]$	σ_x/ρ_1	$\sigma_{\zeta_{\mathrm{ID}}}/\rho_2$
True	2.5	0.67	1.8	18	0.2	4.5		
CONV	50	0.91	2.81	4.67	0.28	14.39		
ID	7.75	0.91	1.12	4.94	1e-6	6.16	1.3e-3	1.0
OD	4.23	0.7	1.58	14.84	0.22	8.48	0.99	0.99

CONV estimated the parameters very poorly. Especially, C_{w} and A_{win} are overestimated. This is because it has to explain input and output relationship without the heat gain information, and the only way of doing this is to adjust the physical parameters. Specifically, the large unmeasured disturbance during occupied time is compensated by the overestimation in solar heat gain (A_{win}), and then, it is stored into the thermal mass (C_{w}) to explain the unmeasured disturbance during unoccupied time. This mechanism outputs unrealistic parameters as shown in Table 1.

Unlike CONV, ID and OD algorithms have another degree of freedom to explain the input and output relationship without the heat gain information, which is the parameters associated with the disturbance models. Therefore, in overall, the inclusion of the disturbance dynamic gives better parameter estimation under unmeasured disturbances. The ID gives better results in C_{w} and A_{win} as it includes disturbance dynamics, but it under estimates R_{zo}. This can be interpreted that the large unmeasured disturbance is successfully explained by the ID. However, the abrupt changing nature of unmeasured input disturbance (i.e., between occupied and unoccupied time) is not fully captured by the ID dynamics. Consequently, the decrease in unmeasured disturbance during the unoccupied time is compensated by underestimation of R_{zo} giving more heat loss to outdoor air. On the other hand, the OD gives better estimation in most of parameters including C_{w} and R_{zo}, albeit not precisely accurate. As stated in [3], this can be attributed to the noisy nature of input disturbance compared to output disturbance: input disturbance likely has more oscillations and abrupt changes, i.e., high power spectrum for a high frequency region while the output disturbance likely has high power spectrum for a lower frequency region.

Since all the methods show deviations from the True system, it is important to understand how much each method captures the building thermal dynamics and the potential issues being used for prediction applications. In Fig. 3, Bode magnitude plots of different approaches are compared with the True model. In general, the OD shows better performance than the other approaches, and the CONV and the ID approaches failed to capture low-frequency range for $\dot{Q}_{\mathrm{HC}}$. It is noted that all models have good behavior in the high-frequency range for $\dot{Q}_{\mathrm{hc}}$, which indicates the short-term behavior of cooling or heating inputs can be captured.

The step response of measured disturbances (T_{oa} and $\dot{q}_{\mathrm{sol,win}}$) and control input ($\dot{Q}_{\mathrm{hc}}$) for the approaches during 12 hours are compared with the True system in Fig. 4. Overall, the OD shows better performance of capturing the true system dynamics under unmeasured disturbances. For the control input, the CONV and the OD show good performance till 1 hour, but the CONV's performance quickly decreases while OD shows relatively moderate decreases.

In Fig. 5, the indoor temperature predictions with unmeasured disturbance ($\dot{Q}_{\mathrm{gain}}$) as an input are compared to the True model for each method. As expected, the OD's prediction shows better performance compared to the CONV and the ID because the OD's identified parameters are the clos-

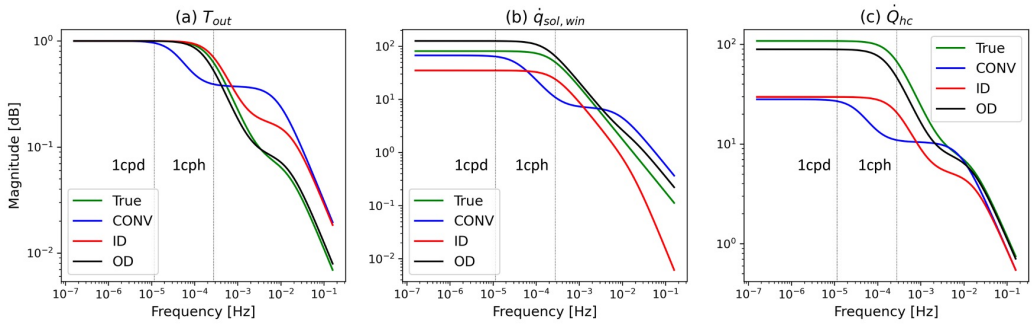

Figure 3: Comparison of Bode magnitude plots of measured disturbances (T_{oa} and $\dot{q}_{\mathrm{sol,win}}$) and control input ($\dot{Q}_{\mathrm{hc}}$) for each method. (1 cph = 2.8e-4 Hz, 1 cpd = 1e-5 Hz)

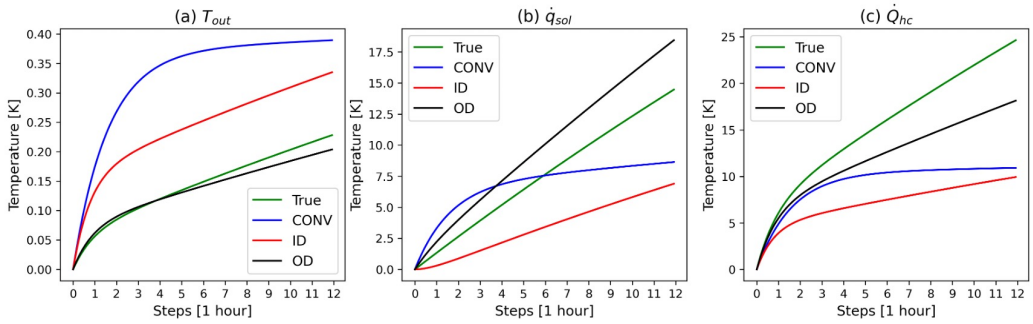

Figure 4: Comparison of step response of measured disturbances (T_{oa} and $\dot{q}_{\mathrm{sol,win}}$) and control input ($\dot{Q}_{\mathrm{hc}}$) for each method.

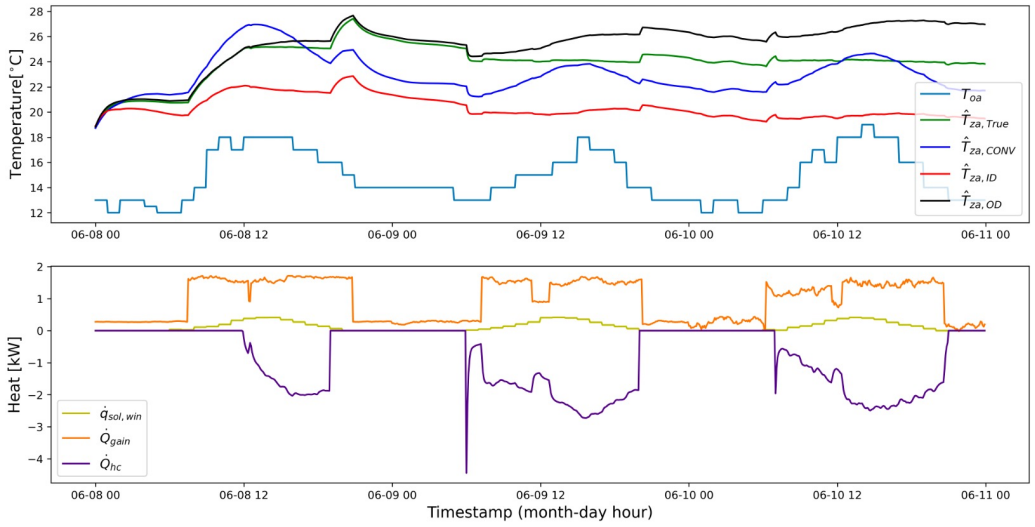

Figure 5: Comparison of indoor temperature predictions with unmeasured disturbance as an input for each method.

est to the True model. However, after the first day, even the OD model over-predicts because some disturbance information is included in the OD parameters as mentioned earlier. The CONV's prediction shows fluctuations as all the unmeasured disturbance information (i.e., fluctuating profiles according to the occupied/unoccupied times) is included in its parameters. But, the ID under-predicts because the ID dynamics majorly captures the large unmeasured disturbance.

Since the indoor temperature is slowly changing dynamics, the required amount of heating or cooling rate to maintain the measured temperature is also a good metric to evaluate how well the model captures the thermal dynamics of the building. For this purpose, the model in Eqs. 1-2 was rewritten as below Eq. 14. After discretizing the system in Eqs. 1-2, the required amount of heating or cooling rate can be estimated assuming the steady state for each sampling time.

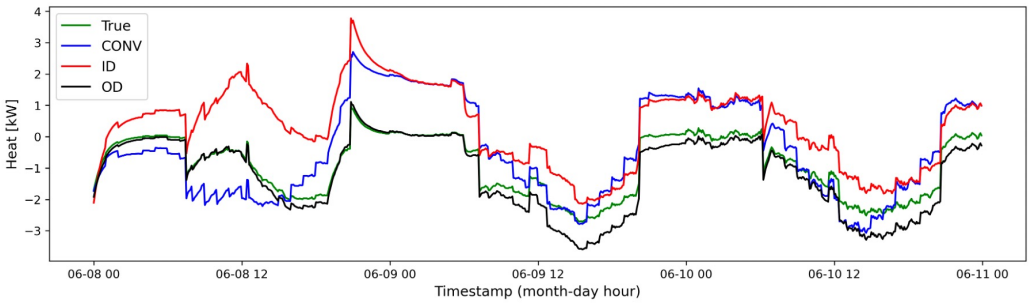

Figure 6: Comparison of required heating or cooling rate to maintain the measured temperature.

$$
\begin{aligned}
\left[\dot{T}_{\mathrm{w}}\right] &= \left[\tfrac{-1}{C_{\mathrm{w}}R_{\mathrm{zw}}}\right]\left[T_{\mathrm{w}}\right] + \begin{bmatrix} 0 & \frac{(1-f)A_{\mathrm{win}}}{C_{\mathrm{w}}} & 0 & \frac{1}{C_{\mathrm{w}}R_{\mathrm{zw}}} \end{bmatrix} \begin{bmatrix} T_{\mathrm{oa}} \\ \dot{q}_{\mathrm{sol,win}} \\ \dot{Q}_{\mathrm{hc}} \\ T_{\mathrm{za}} \end{bmatrix} \\
\dot{Q}_{\mathrm{hc}}(k) &= \frac{T_{\mathrm{za}}(k) - T_{\mathrm{w}}(k)}{R_{\mathrm{zw}}} \\
&\quad + \frac{T_{\mathrm{za}}(k) - T_{\mathrm{oa}}(k)}{R_{\mathrm{zo}}} - fA_{\mathrm{win}}\dot{q}_{\mathrm{sol,win}}(k) - \dot{Q}_{\mathrm{gain}}(k)
\end{aligned}
\tag{14}
$$

In Fig. 6, the amounts of required heat during each sampling time to maintain the measured temperature are compared. Similar to the temperature prediction, the OD shows little over-cooling while the ID shows under-cooling, and the CONV shows both over- and under-cooling. From the two analysis in Figs. 5-6, all the methods include the dynamics of unmeasured disturbance in their parameters to some extent while the OD includes the least.

3. Conclusion

To develop a low-cost and scalable Model Predictive Control (MPC), it is crucial to minimize sensor requirements for both modeling and control implmentations, particularly for small and medium-sized commercial buildings (SMCBs). However, the limited building information resulting from minimal sensor requirements poses challenges across various stages of MPC design, spanning from modeling to control implementation. In this final report, new

modeling approaches have been proposed and evaluated through simulations. The standout feature of these modeling approaches, as compared to conventional methods in the field of building control, is their capacity to extract an improved thermal network model for buildings from imperfect measurements. The algorithm is expected to overcome technical challenges and offer an enhanced MPC model. This enhancement will enable the realization of a low-cost and scalable MPC solution for applications in SMCBs.

References

[1] J. Braun, N. Chaturvedi, An inverse Gray-Box model for transient building load prediction, HVAC&R Research 8 (1) (2002) 73–99. doi:10.1080/10789669.2002.10391290.

[2] X. Li, J. Wen, Review of building energy modeling for control and operation, Renewable and Sustainable Energy Reviews 37 (2014) 517–537. doi:10.1016/j.rser.2014.05.056.

[3] D. Kim, J. Cai, K. B. Ariyur, J. E. Braun, System identification for building thermal systems under the presence of unmeasured disturbances in closed loop operation: Lumped disturbance modeling approach, Building and environment 107 (2016) 169–180. doi:10.1016/j.buildenv.2016.07.007.

[4] D. Kim, J. Cai, J. E. Braun, K. B. Ariyur, System identification for building thermal systems under the presence of unmeasured disturbances in closed loop operation: Theoretical analysis and application, Energy and Buildings 167 (2018) 359–369. doi:10.1016/j.enbuild.2017.12.007.

[5] A. R. Coffman, P. Barooah, Simultaneous identification of dynamic model and occupant-induced disturbance for commercial buildings, Building and environment 128 (2018) 153–160. doi:10.1016/j.buildenv.2017.10.020.

[6] P. Radecki, B. Hencey, Online model estimation for predictive thermal control of buildings, IEEE Transactions on Control Systems Technology 25 (4) (2017) 1414–1422. doi:10.1109/TCST.2016.2587737.

[7] Lawrence Berkeley National Laboratory, FLEXLAB the world's most advanced integrated building and grid technologies testbed, https://flexlab.lbl.gov/, accessed: 2021-12-24 (2021).

[8] U.S. Department of Energy, EnergyPlus - weather data, https://energyplus.net/weather-location/north_and_central_america_wmo_region_4/USA/CA/USA_CA_Oakland.Intl.AP.724930_TMY3, accessed: 2021-12-24 (2021).

[9] S. Rouchier, M. J. Jiménez, S. Castaño, Sequential monte carlo for online parameter estimation of a lumped building energy model, Energy and Buildings 187 (2019) 86–94. doi:10.1016/j.enbuild.2019.01.045.